

## Collective excitations in imperfect parabolic quantum wells with in-plane magnetic fields

P. I. Tamborenea and S. Das Sarma

*Department of Physics, University of Maryland, College Park, Maryland 20742-4111*

(Received 7 July 1993; revised manuscript received 25 January 1994)

Calculations of far-infrared optical absorption for  $\text{Al}_x\text{Ga}_{1-x}\text{As}$  perturbed parabolic quantum wells (PQW) with a magnetic field in the plane of the electron slab are presented within the linear response theory. The nonparabolicities associated with the perturbation allow the coupling of long-wavelength radiation to collective excitations of the electron gas other than the center-of-mass mode, otherwise forbidden in pure PQW's by virtue of Kohn's theorem. We employ a quantum-mechanical self-consistent-field approach which makes use of the density functional formalism within the local-density approximation. We study two different types of samples employed in recent magneto-optical absorption measurements. The first consist of PQW's with controlled  $\delta$ -planar perturbations located at the center of the well or forming superlattice-like periodic arrays. These samples were recently used in an experimental study aimed at indirectly measuring the magnetoroton dispersion relation of a three-dimensional electron gas. We construct a magnetoplasma dispersion relation and critically discuss whether the experimental results are consistent with the bulk magnetoroton picture originally invoked to understand the data. The second system we study is asymmetric parabolic wells, obtaining good agreement with experiment at high and low areal densities, but quantitative discrepancies at intermediate density.

### I. INTRODUCTION

Remotely doped  $\text{Al}_x\text{Ga}_{1-x}\text{As}$  parabolic quantum wells (PQW's) are systems where a wide, high-mobility quasi-two-dimensional (2D) electron gas can be realized.<sup>1</sup> Such systems have been proposed as candidates for the observation of three-dimensional electron-electron interaction effects in an environment free of impurities.<sup>2</sup> The generalized Kohn theorem,<sup>3</sup> which states that an electron gas in perfect parabolic confinement with a magnetic field applied in an arbitrary direction absorbs long-wavelength light at the two frequencies that correspond to excitations in the center-of-mass (CM) motion, fully explained the results of far-infrared (FIR) optical absorption experiments in perfect PQW's. It then became clear that this type of experiment could reveal characteristics of the electron-electron interaction only if slight imperfections were introduced in the parabolic confinement. Since then a number of imperfect parabolic well systems have been investigated experimentally<sup>4-6</sup> and theoretically, without magnetic fields,<sup>7</sup> and with tilted<sup>8</sup> and in-plane magnetic fields.<sup>9</sup>

In this paper we will present theoretical calculations related to recent FIR absorption experiments on imperfect parabolic wells in the Voigt geometry, i.e., with a magnetic field  $\vec{B}$  applied in the plane of the electron slab and radiation propagating perpendicular to that plane with polarization  $\vec{E}^{\text{rad}} \perp \vec{B}$ . For pure parabolic wells in this geometry there is only one resonance (the so-called Kohn mode) at the frequency  $\omega_K = (\omega_0^2 + \omega_c^2)^{1/2}$ , independent of the areal density  $N_s$ , as stated by the generalized Kohn theorem. In this expression  $\omega_0 = (2\alpha_0/m^*)^{1/2}$  is the frequency of the harmonic confining potential

$V_{\text{conf}} = \alpha_0 z^2$ ,  $m^*$  is the electron effective mass in GaAs, and  $\omega_c = (eB/m^*c)^{1/2}$  is the cyclotron frequency. This center-of-mass mode is the only one that couples to long-wavelength radiation and corresponds to a rigid oscillation of the electron slab. By introducing controlled perturbations on PQW samples it becomes experimentally possible to study nonuniform modes of oscillation of the (quasi)parabolically confined electron gas, which make manifest the internal degrees of freedom of this many-body system.

An interesting application<sup>5</sup> of the idea of using a wide PQW to study the properties of a 3D electron gas in a strong magnetic field is the recent measurement of FIR spectra of samples with controlled  $\delta$ -planar perturbations (thin layers of  $\text{Al}_x\text{Ga}_{1-x}\text{As}$  with a different concentration of aluminum which produce small spikes in the otherwise parabolic potential). Besides the expected Kohn mode, additional peaks appeared in the spectra, which, interpreted as collective excitations with a certain transversal wave vector  $q_z$  (to be suitably defined), permitted the construction of a "three-dimensional" magnetoplasmon dispersion relation. The result showed a minimum around  $q_z = 2/\ell_c$  ( $\ell_c$  is the magnetic length) in agreement with the magnetoroton minimum predicted by the 3D calculation in the single-mode approximation.<sup>5</sup> In this paper we apply the insight provided by a microscopic quantum-mechanical calculation that takes into account the exact geometry of the experimental samples to test the validity of the assumptions underlying the interpretation of the experimental data made in Ref. 5.

A simple departure from perfect parabolicity is given by the case of an asymmetric parabolic well consisting of two half parabolas of slightly different curvatures. FIR magneto-optical absorption experiments were re-

cently realized in such a system.<sup>6</sup> The spectra showed a crossover from a quantum regime with  $N_s/\bar{n}_0 \ll \ell_c$  ( $\bar{n}_0$  is the average design density) to a classical regime with  $N_s/\bar{n}_0 \gg \ell_c$ . The crossover region over which a unique resonance (at low  $N_s$ ) splits into two ‘‘Kohn modes’’ (at high  $N_s$ ) is roughly given by the condition  $2\ell_1 < N_s/\bar{n}_0 < 4\ell_1$ , where  $\ell_1 = \sqrt{3}\ell_c$  is the radius of the second Landau orbit. Here we calculate absorption spectra for an asymmetric PQW modeled following the parameter values of the sample used in Ref. 6 and compare our results with experiment in the relevant range of areal densities.

The outline of the rest of the paper is as follows. In Sec. II we describe the method employed in our calculation of long-wavelength optical absorption in the Voigt geometry. In Sec. III we present the results for the samples employed in the experimental construction of the magnetoroton dispersion relation. The asymmetric parabolic well problem is covered in Sec. IV, and in Sec. V we provide some concluding remarks.

## II. METHOD

Intersubband optical absorption for a quasi-2D electron gas in the presence of an in-plane magnetic field with the radiation polarized in the growth direction has been calculated by Ando,<sup>10</sup> and his treatment was adapted to the normal incidence case by Dempsey and Halperin.<sup>9</sup> In this article we employ a similar self-consistent-field approach, which includes exchange and correlation effects within the local-density approximation (LDA). We choose the  $z$  axis to be in the confinement direction, the magnetic field  $\vec{B} = (0, B, 0)$ , and the gauge  $\vec{A} = (Bz, 0, 0)$ . Ignoring the Zeeman energy for simplicity, and working in the effective mass approximation, we write the effective single-particle Hamiltonian as

$$H = \frac{(p_x + m^* \omega_c z)^2}{2m^*} + \frac{p_y^2}{2m^*} + \frac{p_z^2}{2m^*} + V_{\text{eff}}(z), \quad (1)$$

where the effective confining potential  $V_{\text{eff}}(z) = V_{\text{conf}} + V_H(z) + V_{\text{XC}}(z)$  contains contributions from the bare confining potential, the Hartree potential, and the exchange-correlation potential within the local-density approximation.<sup>11</sup> The eigenfunctions of  $H$  are factorized as

$$\psi_{nk_x k_y}(x, y, z) = \frac{e^{ik_x x}}{L_x^{1/2}} \frac{e^{ik_y y}}{L_y^{1/2}} \varphi_{nk_x}(z), \quad (2)$$

and the corresponding eigenenergies are  $E_n(k_x, k_y) = \frac{\hbar^2 k_y^2}{2m^*} + \varepsilon_n(k_x)$ . Notice that in the presence of an in-plane magnetic field the  $z$ -dependent part of the solution of the eigenvalue problem also depends on  $k_x$ , making the dispersion  $\varepsilon_n(k_x)$  nonparabolic, and thereby the calculation of the self-consistent electronic structure computationally demanding. In this work, the quasicontinuous set of values of the quantum number  $k_x$  obtained when periodic boundary conditions are applied in the  $x$  direction

is discretized into a coarser mesh to make the problem tractable numerically.<sup>10,12,9</sup> The self-consistent density is given by

$$n(z) = \sum_{nk_x} N_{nk_x} |\varphi_{nk_x}(z)|^2, \quad (3)$$

where  $N_{nk_x}$  is the occupancy of the single-particle states labeled with  $(n, k_x)$ . We restrict our treatment to zero temperature. Next we make use of the self-consistent electronic structure and time-dependent perturbation theory to calculate the linear response of the system to long-wavelength radiation. The  $zz$  component of the modified two-dimensional conductivity is given by

$$\tilde{\sigma}_{zz}^{2D} = -i\omega e^2 \sum_{\eta} \frac{f_{\eta}^{(z)}}{\tilde{\varepsilon}_{\eta}^2 - (\hbar\omega)^2 - 2i\hbar^2\omega/\tau}, \quad (4)$$

where  $\tilde{\varepsilon}_{\eta}$  are the resonant energies, which include the depolarization and the excitonlike corrections,<sup>10,13</sup>  $\tilde{f}_{\eta}^{(z)}$  are the corresponding oscillator strengths, and  $\tau$  is a phenomenological relaxation time. If only the lowest subband is occupied in the Voigt configuration, the index  $\eta$  has a one-to-one correspondence to the composite index  $(n, k_x)$ . Since the radiation is normally incident, the absorbed power is proportional to the real part of the  $xx$  component of  $\tilde{\sigma}^{2D}$ , which is given by  $\text{Re}[\tilde{\sigma}_{xx}^{2D}] = \frac{\omega^2}{\omega^2} \text{Re}[\tilde{\sigma}_{zz}^{2D}]$ .<sup>9</sup> We will also need to calculate the density fluctuations associated with the resonant modes of the electron gas. For the resonant mode  $\eta$  we obtain

$$\delta n_{\eta}(z) \propto \sum_{n, k_x} \varepsilon_{n0}(k_x) N_{nk_x}^{1/2} \varphi_{nk_x}(z) \varphi_{0k_x}(z) U_{nk_x, \eta}, \quad (5)$$

where  $\varepsilon_{n0}(k_x) \equiv \varepsilon_n(k_x) - \varepsilon_0(k_x)$ , and  $U_{nk_x, \eta}$  is a unitary matrix used in the linear response calculation leading to Eq. (4), whose eigenvalues are  $\tilde{\varepsilon}_{\eta}^2$ . More details on the technical aspects of these calculations can be found in the literature.<sup>8-12</sup>

## III. PARABOLIC WELLS WITH $\delta$ PERTURBATIONS

### A. Introduction

Recently, the magneto-optical spectra of a quasi-2D electron gas confined in wide PQW's with  $\delta$ -planar perturbations has been measured.<sup>5</sup> The perturbations were deliberately grown in the PQW samples to ‘‘violate’’ the generalized Kohn theorem and thereby allow the coupling of long-wavelength radiation to the internal modes of oscillation of the electron gas. By assigning wave vectors  $q_z = \frac{N\pi}{W}$ , or  $q_z = \frac{2\pi}{a}$  ( $W =$  width of the electron slab,  $a =$  spike separation in the  $\delta$ -array samples), corresponding to dimensional resonances in the direction of confinement, it was possible to construct a dispersion relation for the magnetoplasma excitations in the electron gas. In this way, in Ref. 5 the experimental data were interpreted as the observation of a 3D magnetoroton minimum in the magnetoplasmon dispersion of a quasi-2D

electron gas. We emphasize the important conceptual distinctions between our calculations and the theoretical interpretation used in the original work of Ref. 5. We consider the *actual* experimental system which is a PQW quasi-2D electron gas with only a few quantum subbands occupied in the zero field (and only *one* magnetosubband populated under the magnetic field values used in the experiment) whereas in Ref. 5 the system was taken to be a purely 3D electron gas. We feel that the 3D approximation could apply<sup>14</sup> only when many subbands are occupied, and, more importantly, only if our quasi-2D calculations support such a 3D picture. Our calculation is a fully self-consistent quasi-2D time-dependent local-density approximation (TDLDA), which takes into account the detailed electronic structure of the system (including the  $\delta$  function or the superlattice perturbations), whereas in Ref. 5 a 3D single-mode approximation was used. Finally, and this is a significant but subtle difference, our calculation is in the quasi-2D long-wavelength limit (because the wave vector associated with the incident far-infrared radiation is effectively zero), whereas in Ref. 5 the bulk collective mode is taken to be excited at a finite 3D wave vector defined by the dimensional resonance  $q_z = \frac{N\pi}{W}$ , etc. Note that for the confined quasi-2D PQW system  $q_z$  is not a well-defined concept for the collective modes.

The purpose of our study, thus, is twofold. On the one hand, we intend to compare FIR absorption spectra calculated within the TDLDA with experimental results for parabolic wells with controlled superimposed perturbations in the electrostatic confining potential. This complements other theoretical studies of different types of deviations from perfect parabolicity available in the literature.<sup>8,9,12</sup> On the other hand, we examine the validity of constructing a 3D magnetoplasmon dispersion relation from the information provided by the confined intersubband excitations. We do so by calculating the microscopic density fluctuations associated with the various observable collective modes, and using them to introduce a simple definition of the “fictitious” wave vectors  $q_z$ . Ours is a generalization to the magnetic field case of the method of Teich and Mahler,<sup>14</sup> whose results provided the heuristic basis for the analysis of the experimental data employed in Ref. 5.

### B. Magneto-optical absorption spectra

In Fig. 1(a) we show our model bare potential for the PQW sample with a single  $\delta$ -planar perturbation studied experimentally in Ref. 5. The peak in the middle of the well is taken to have a Gaussian shape, and its strength is about six times larger than the value specified for the real sample. Also shown in Fig. 1(a) are the self-consistent potentials for the minimum and maximum areal densities used in the experiment,  $N_s = 1.64 \times 10^{11} \text{ cm}^{-2}$  and  $2.24 \times 10^{11} \text{ cm}^{-2}$ , with an applied in-plane magnetic field of  $B = 5.4 \text{ T}$ . Given that the location of the  $\delta$  peak is known in the experiment only within 10% of the well width,<sup>15</sup> we also consider a PQW with a slightly off-centered  $\delta$ -planar perturbation. The model

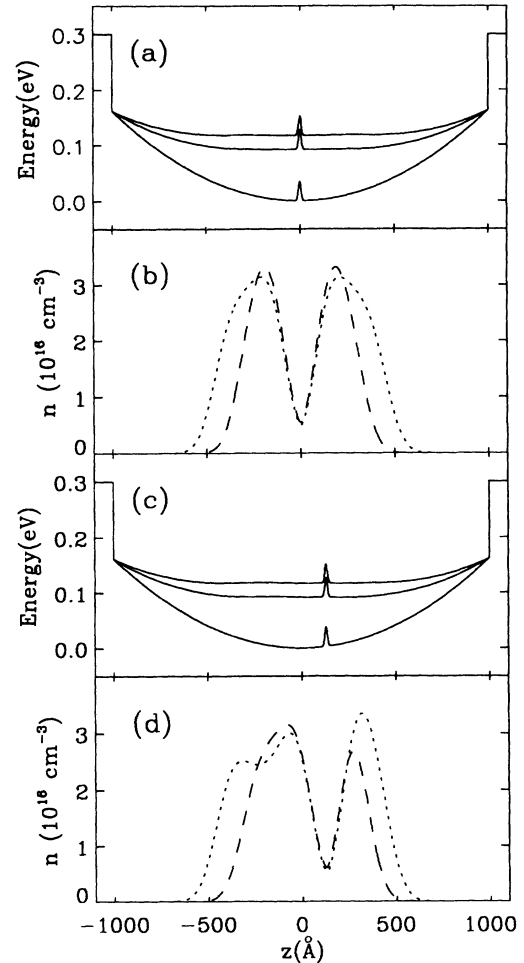


FIG. 1. Model bare potential of the parabolic well with (a) a centered and (c) an off-centered  $\delta$ -planar perturbation (bottom line), and calculated self-consistent potentials with an in-plane magnetic field of  $B = 5.4 \text{ T}$ , for  $N_s = 1.64$  (middle line) and  $2.24 \times 10^{11} \text{ cm}^{-2}$  (top line); (b) and (d) show the calculated self-consistent densities corresponding to the potentials of (a) and (c), respectively, for  $N_s = 1.64$  (dashed line) and  $2.24 \times 10^{11} \text{ cm}^{-2}$  (dotted line).

PQW with a perturbation slightly displaced from the center of the well is shown in Fig. 1(c). The displacement is  $130 \text{ \AA}$ , somewhat larger than the magnetic length  $\ell_c = (\frac{\hbar c}{eB})^{1/2} \approx 110 \text{ \AA}$ , but less than 10% of the well width. The ground-state self-consistent electronic densities corresponding to our two model potentials are shown in Figs. 1(b) and (d).

The absorption spectra for the PQW with a centered spike are shown in Fig. 2. At both densities we observe a strong peak corresponding approximately to the CM mode (Kohn mode) of frequency  $\omega_K$  characteristic of perfect PQW's, in agreement with experiment. In our calculation the frequencies of these resonances are shifted away from  $\omega_K$ , but the analogy with the CM mode is corroborated by the shape of their density fluctuations, which are approximately proportional to the derivative of the ground-state density  $\frac{dn}{dz}$  [see Fig. 3(a)] as occurs in

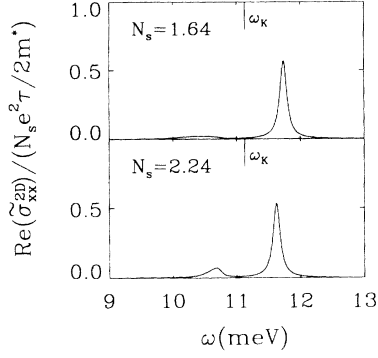


FIG. 2. Calculated absorption spectra for the parabolic well with a centered  $\delta$ -planar perturbation, with a magnetic field  $B = 5.4$  T in the Voigt geometry for two different areal densities  $N_s$  (given in units of  $10^{11} \text{ cm}^{-2}$ ). The “Kohn” frequency  $\omega_K = (\omega_0^2 + \omega_c^2)^{1/2}$  associated with the curvature of the well is shown as a reference.

the center-of-mass motion. To decide whether the positions of the secondary resonances agree with experiment we need to consider that, while our results are shown as functions of the resonant frequency, the transmission experiments were performed sweeping the magnetic field at a constant radiation frequency. Since the resonant frequencies increase monotonically with magnetic field [approximately as  $\omega \approx (\omega_0^2 + \omega_c^2)^{1/2}$ ], an absorption peak falling on the low-frequency side of the CM resonance in the calculated spectrum corresponds to a transmission peak on the high-magnetic-field side of the CM resonance in the experimental spectrum. We therefore verify that the relative positions of the secondary resonances in our calculation agree with those of the experiment. There is also agreement in the fact that both in theory and experiment the separation between the main and the secondary peaks decreases with increasing  $N_s$ . However, the theoretical separations,  $\Delta\omega_{\text{calc}} = 1.32$  and  $1.0$  meV for  $N_s = 1.64$  and  $2.24 \times 10^{11} \text{ cm}^{-2}$ , respectively, are about a factor of 3 larger than the experimental values  $\Delta\omega_{\text{exp}} = 0.48$  and  $0.32$  meV. Another discrepancy appears in the intensities of the secondary resonances: in the calculation, the secondary resonance at low  $N_s$  has less oscillator strength than the one at higher  $N_s$ , contrary to the experimental finding. A better agreement on these points will be found with the model potential with an off-centered spike.

Our calculations of the dynamical conductivity for the PQW with a centered  $\delta$ -planar perturbation show a collective mode whose frequency lies between the two resonances observed in the spectra of Fig. 2, but with zero oscillator strength. This collective mode does not give rise to power absorption because the density fluctuations associated with it are symmetric with respect to  $z = 0$ , as shown in Fig. 3(b), and therefore cannot couple to long-wavelength radiation. In the model potential with an off-centered  $\delta$ -planar perturbation the symmetry of the Hamiltonian is broken, and therefore such collective modes become visible in the absorption spectrum. The middle peaks in Fig. 4 correspond to the formerly forbidden symmetric modes, as can be verified from the form

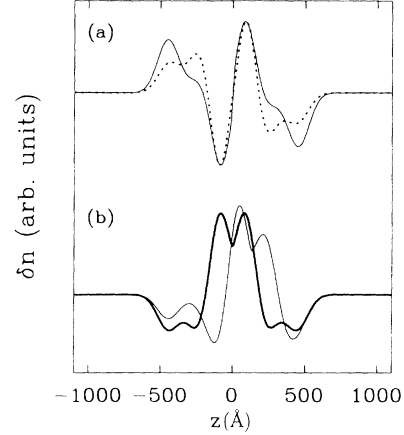


FIG. 3. (a) Density fluctuations  $\delta n(z)$  (dotted line) associated with the shifted “Kohn mode” for the potential with a centered  $\delta$ -function perturbation, at  $N_s = 2.42 \times 10^{11} \text{ cm}^{-2}$ , and the derivative of the equilibrium density  $\frac{dn}{dz}$  (solid line). (b) The symmetry-disallowed mode of the centered  $\delta$ -function potential (thick line) and the corresponding resonant mode for the off-centered  $\delta$ -function potential (thin line).

of their density fluctuation profiles [Fig. 3(b)]. A comparison of the separations between the main resonance and the secondary ones gives now a substantially better agreement than with the centered perturbation. For  $N_s = 1.64 \times 10^{11} \text{ cm}^{-2}$ ,  $\Delta\omega_{\text{calc}} = 0.43$  meV, whereas  $\Delta\omega_{\text{exp}} = 0.48$  meV, and for  $N_s = 2.24 \times 10^{11} \text{ cm}^{-2}$ ,  $\Delta\omega_{\text{calc}} = 0.22$  meV for the first peak and  $0.86$  meV for the second one, whereas  $\Delta\omega_{\text{exp}} = 0.32$  meV and  $0.71$  meV, respectively.

We have also performed calculations of optical absorption spectra for a parabolic well with a periodic array of  $\delta$ -planar perturbations with a distance between spikes  $a = 300$   $\text{\AA}$ . Using spike strengths ten times larger than in the experiment, we obtain a broad secondary peak whose energy is approximately equal to the cyclotron energy for two different areal densities. Consequently, its separation to the Kohn mode is independent of  $N_s$ , in qualitative agreement with the experimental spectra. However, this

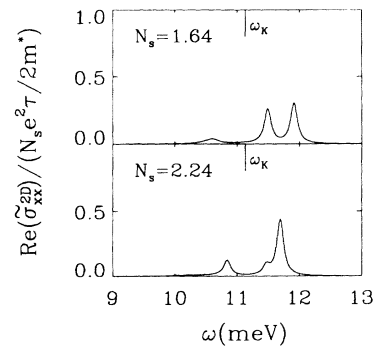


FIG. 4. Calculated absorption spectra for the parabolic well with an off-centered  $\delta$ -planar perturbation, with a magnetic field  $B = 5.4$  T in the Voigt geometry for two different areal densities  $N_s$  (given in units of  $10^{11} \text{ cm}^{-2}$ ). The “Kohn” frequency  $\omega_K = (\omega_0^2 + \omega_c^2)^{1/2}$  associated with the curvature of the well is shown as a reference.

resonance is weaker than the experimental one, and its energy difference with the Kohn mode is somewhat larger than in the experiment. For a parabolic well with a periodic array of  $\delta$ -planar perturbations with a distance between spikes  $a = 200 \text{ \AA}$ , we also obtain a broad resonance around the cyclotron frequency. It should be emphasized, however, that the precise forms of the perturbations in the experimental samples are, in general, unknown and, under the circumstances, our approximately quantitative agreement with experiment is all we can hope for.

### C. Construction of a magnetoplasmon dispersion relation

In this section we examine the basic assumption made in the interpretation of the experimental data of Ref. 5, which made possible the construction of a “bulk” dispersion relation out of the measured energies of the confined intersubband collective excitations. This connection was established by assuming that the different resonances observed experimentally correspond approximately to sinusoidal standing waves in the electron density with wave vectors  $q_z = \frac{N\pi}{W}$ , or  $q_z = \frac{2\pi}{a}$ , where  $W = N_s/n_0$  is the approximate width of the electron slab ( $n_0$  is the design density of the parabolic well),  $N$  is an even integer, and  $a$  is the periodicity of the array of  $\delta$  spikes in the confining potential. This picture was motivated by the following points: (i) the fact that for perfect parabolic wells the ground-state density profile is very uniform over most of the extent of the electron slab, and the assumption that such a uniform equilibrium density would not be substantially altered by the introduction of small perturbations; (ii) random-phase approximation (RPA) calculations in square wells without magnetic fields, which show a remarkable agreement between the bulk plasmon dispersion relation and a dispersion relation constructed from intersubband excitation energies in a similar fashion; and (iii) a hydrodynamic model calculation for perfect parabolic quantum wells in the presence of a magnetic field.<sup>16</sup>

We employed the density fluctuations [see Eq. (5)] associated with the various secondary resonances described in the previous section, whose energies show a semiquantitative agreement with experiment, to construct a dispersion relation with two different definitions of the transverse wave vector  $q_z$ . [An example of such density fluctuations is shown in Fig. 3(b).] We introduce a simple definition of the wave vector in the  $z$  direction,  $q_z = 2\pi/\lambda$ , where  $\lambda \equiv 2W_{\delta n}/(M+1)$ ,  $W_{\delta n}$  is the width of the density fluctuations, and  $M$  is the number of nodes. The resulting dispersion relation is shown as empty symbols in Fig. 5. We plot the same data points with  $q_z$  defined as in Ref. 5 as solid symbols. As a caveat we mention that the four points with smaller  $q_z$  have been shifted down in energy by an amount equal to the displacement of the Kohn modes from their theoretical values. This correction seems justified since we verified that the same potentials with smaller spikes do not have their Kohn modes displaced from the expected values. The solid line is the 3D RPA magnetoplasmon dispersion.<sup>17</sup> It can

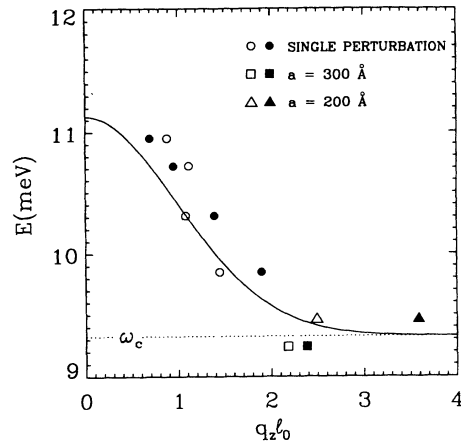


FIG. 5. Magnetoplasmon dispersion relation constructed by assigning simply defined transverse wave vectors  $q_z$  to the intersubband charge density excitations of various PQW's with  $\delta$ -planar perturbations. Open symbols correspond to the  $q_z$  extracted from the calculated density fluctuations, and solid symbols correspond to the definitions of  $q_z$  used in Ref. 5 (see text). The solid line gives the bulk RPA magnetoplasmon dispersion at a 3D density equal to the design density of the PQW.

be seen that the two definitions of  $q_z$  give a reasonable agreement with each other and with the bulk RPA result. Therefore, our analysis supports, at least qualitatively, the method used in Ref. 5 to relate the FIR absorption data to the 3D single-mode approximation calculation. However, we feel that this type of interpretation of the long-wavelength quantum-confined quasi-2D collective intersubband charge density excitation modes should be taken with caution, due to the ambiguity in the definition of the transverse wave vectors  $q_z$ . At this stage we can at most say that such an interpretation would be meaningful only if it were backed by a microscopic calculation that takes into account the exact geometry of the problem, like the one presented here.

### IV. ASYMMETRIC PARABOLIC WELLS

In this section we present results for the asymmetric parabolic well studied experimentally in Ref. 6. The aim of that study was to determine the conditions for a quasi-2D electron gas to cross over from two- to three-dimensional behavior. The FIR magneto-optical spectra evolve, as the areal density increases (and with it, the width of the electron slab), from one peak at the inter-Landau-level energy difference of the bare well to two peaks located at the Kohn frequencies of the half parabolas. As we mentioned in the Introduction, there is a crossover region given approximately by  $2\ell_1 < N_s/\bar{n}_0 < 4\ell_1$ , where  $\ell_1 = \sqrt{3}l_c$ . The upper limit shows that to obtain two separate resonances at the Kohn frequencies the slab has to be wide enough to accommodate one excited Landau orbit in each half of the well.

We consider the model potential shown in Fig. 6(a) to describe the asymmetric PQW sample studied in Ref.

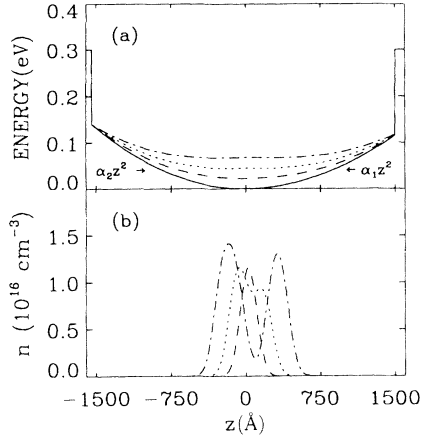


FIG. 6. (a) Model bare potential of the asymmetric parabolic well (solid line), and calculated self-consistent potentials with an in-plane magnetic field of  $B = 5.8$  T, for  $N_s = 2.4$  (dashed line), 4.7 (dotted line), and  $7.5 \times 10^{10} \text{ cm}^{-2}$  (dash-dotted line); (b) corresponding calculated self-consistent densities.

6. It consists of two half parabolas with curvatures  $\alpha_1 = 5.1 \times 10^{-5} \text{ meV}/\text{Å}^2$  and  $\alpha_2 = 6.2 \times 10^{-5} \text{ meV}/\text{Å}^2$ , and is  $3000 \text{ Å}$  wide. We choose a magnetic field in the region of the observed resonances of  $B = 5.8$  T. In Fig. 6(a) we show the calculated self-consistent potentials for some values of the sheet density  $N_s$ , which, as expected, become flattened over a wider region in the center of the well as the electron slab width increases with  $N_s$ . Note, however, that the density profiles  $n(z)$  shown in Fig. 6(b) are not flat as in the pure parabolic wells, as might have been expected naively. For the values of  $N_s$  considered in the experiment, and in our calculations with magnetic field, only the lowest subband is occupied at zero temperature. We checked that the abrupt change in the curvature at  $z = 0$  does not produce unphysical results by using a similar potential with a graded change in curvature, and the density profile was identical to the original one within our numerical precision.

The optical absorption spectra for the asymmetric quantum well and for several densities  $N_s$  in the range used in Ref. 6 are shown in Fig. 7. The frequencies associated with the half parabolas of curvatures  $\alpha_{1,2}$  are  $\omega_{1,2} = 2\alpha_{1,2}/m^*$ . The frequencies  $\omega_{K1,K2}$  marked for reference on each panel of Fig. 7 are the “Kohn” frequencies of each half parabola,  $\omega_{K1,K2} = (\omega_{1,2}^2 + \omega_c^2)^{1/2}$ . The phenomenological scattering time  $\tau = 20 \times 10^{-12} \text{ s}$ , taken to be a constant in our calculations, was obtained from the linewidth of the narrower resonance in the experiment.<sup>6</sup> For a perfect PQW the generalized Kohn theorem predicts a unique resonance independent of the electron density. In our case, in contrast, we obtain a strong dependence on  $N_s$ . For small  $N_s \lesssim 4.7 \times 10^{10} \text{ cm}^{-2}$  there is only one resonance (for example,  $\tilde{\epsilon} = 10.644 \text{ meV}$  at  $N_s = 0.1 \times 10^{10} \text{ cm}^{-2}$ ), corresponding to the optical transition between the first two energy levels of the bare confining potential in the presence of the in-plane magnetic field, whose energy is  $\epsilon_1(k_x = 0) - \epsilon_0(k_x = 0) = 10.648 \text{ meV}$ .

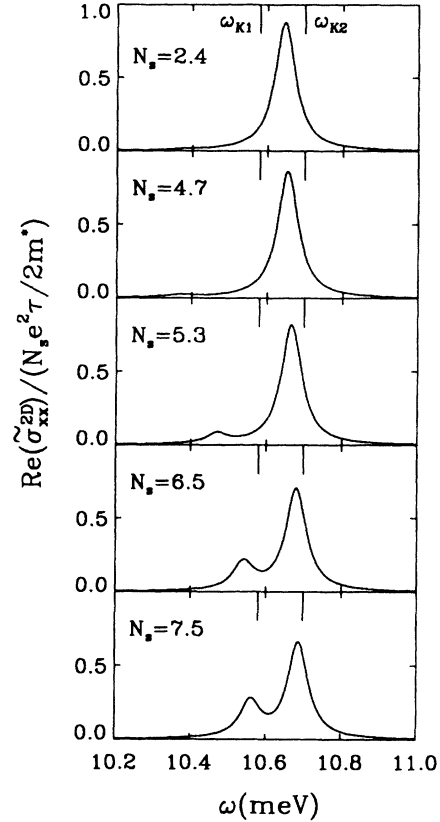


FIG. 7. Calculated absorption spectra for the asymmetric parabolic quantum well with a magnetic field  $B = 5.8$  T in the Voigt geometry for various areal densities  $N_s$  (given in units of  $10^{10} \text{ cm}^{-2}$ ).  $\omega_{K1}$  and  $\omega_{K2}$  are the “Kohn” frequencies associated with the curvatures of the two half parabolas of the well.

As  $N_s$  increases another resonance appears at an energy lower than  $\omega_{K1}$ , and gradually moves to  $\omega_{K1}$  while the other resonance also shifts to end up at  $\omega_{K2}$  for high  $N_s$ . At a sheet density  $N_s = 7.5 \times 10^{10} \text{ cm}^{-2}$  (the highest  $N_s$  reported in the experiment) we obtain two resonances  $\omega_{1,2}^{\text{res}}$  very close to the “Kohn” frequencies  $\omega_{K1,K2}$ . We note that a direct comparison of the theoretical and calculated spectra is not possible because the experimental results correspond to a magnetic field sweep at a constant resonance frequency whereas the calculated optical spectra are given as a function of frequency at a fixed magnetic field. In order to make a quantitative comparison with experiment, we use the resonant frequencies  $\omega_{1,2}^{\text{res}}$  to compute the harmonic oscillator frequencies of the well halves  $\omega_{1,2}^{\text{calc}} = [(\omega_{1,2}^{\text{res}})^2 - \omega_c^2]^{1/2}$ , and obtain their difference  $\omega_2^{\text{calc}} - \omega_1^{\text{calc}} = 0.378 \text{ meV}$ . This shows an 8% discrepancy with the input value  $\omega_2 - \omega_1 = 0.350 \text{ meV}$  ( $\omega_{1,2}$  are the values used in the definition of the confining potential) which is comparable to the 4% discrepancy found in experiment between the design parameters and the observed resonances, at the same sheet density.

Therefore, we obtain a very good agreement with the experimental results of Ref. 6 for low and high  $N_s$ . The agreement at high  $N_s$  also confirms the strong magnetic

field classical arguments based on the Magarill-Chaplik<sup>18</sup> theory given in Ref. 6. At intermediate  $N_s$ , however, the position of the weaker resonance seems to evolve in different ways as a function of  $N_s$  in theory and experiment. In the experiment, the two "Kohn" resonances found at high  $N_s$  appear to merge into one absorption peak as  $N_s$  is reduced, in contrast to the separation and vanishing of one of the resonances found in our calculation. One possibility is that this discrepancy appears as a result of the different types of spectra obtained in theory and experiment (frequency versus magnetic field sweep) and then an improved fit to the experimental results at intermediate  $N_s$  could be obtained if a magnetic-field- and density-dependent scattering time  $\tau(B, N_s)$  is included in the calculation.

## V. CONCLUSION

We have studied theoretically the properties of the collective modes of two types of imperfect parabolic wells as manifested in long-wavelength magneto-optical absorption experiments. Our TDLDA calculations of the spectra for parabolic PQW's with a small perturbation in the middle of the well are in good semiquantitative agreement with experiment. This agreement is considerably improved if the perturbation is placed slightly off centered, in which case formerly symmetry-disallowed modes appear in the spectra. This interpretation could be further investigated experimentally if the position of the  $\delta$ -planar perturbation were varied systematically around the center of the well, thus controlling the strength of

the symmetric mode. We construct a magnetoplasmon dispersion relation by assigning transverse wave vectors  $q_z$  to the inter-Landau-level resonances, which displays a reasonable qualitative agreement with the bulk RPA result. This analysis provides some support for the interpretation of experimental results as the observation of a magnetoroton feature in the magnetoplasmon dispersion relation of a 3D electron gas predicted by a single-mode approximation calculation.<sup>5</sup> We also calculate the absorption spectra of an asymmetric PQW recently studied experimentally.<sup>6,19</sup> A comparison of our results with experiment shows good quantitative agreement with experiment for low and high  $N_s$  but some quantitative discrepancies in the crossover region from two- to three-dimensional behavior. The origin of this disagreement remains an open question. A theory including finite temperatures and a treatment of exchange and correlation that takes into account the presence of the strong magnetic field may be necessary. On the other hand, experiments with a frequency sweep at constant magnetic field would permit a more direct comparison between our calculation and experiment.

## ACKNOWLEDGMENTS

The authors are very much indebted to H. D. Drew for numerous discussions and, particularly, for his patient explanations of different aspects of the experimental work. We also thank Ben Y-K. Hu, I. K. Marmoros, and K. Karrai for useful discussions. This work is supported by the U.S. ARO, U.S. ONR, and the NSF.

<sup>1</sup> S. Das Sarma, in *Topics in Condensed Matter Physics*, edited by M. Das (Nova Science, New York, 1993), and references therein.

<sup>2</sup> B. I. Halperin, *Jpn. J. Appl. Phys.* **26**, Suppl. 26-3, 1913 (1987).

<sup>3</sup> L. Brey, N. F. Johnson, and B. Halperin, *Phys. Rev. B* **40**, 10647 (1989); I. K. Marmoros and S. Das Sarma, *ibid.* **48**, 1544 (1993), and references therein.

<sup>4</sup> A. Wixforth, M. Sundaram, J. H. English, and A. C. Gosard, in *Proceedings of the 20th International Conference on the Physics of Semiconductors*, edited by E. M. Anastassakis and J. D. Joannopoulos (World Scientific, Singapore, 1990), p. 1705.

<sup>5</sup> K. Karrai, X. Ying, H. D. Drew, M. Santos, M. Shayegan, S.-R. E. Yang, and A. H. Mac Donald, *Phys. Rev. Lett.* **67**, 3428 (1991); H. D. Drew, X. Ying, K. Karrai, M. Shayegan, and M. Santos, *Physica B* **184**, 100 (1993).

<sup>6</sup> X. Ying, K. Karrai, H. D. Drew, M. Santos, and M. Shayegan, *Phys. Rev. B* **46**, 1823 (1992).

<sup>7</sup> L. Brey, Jed Dempsey, N. F. Johnson, and B. I. Halperin, *Phys. Rev. B* **42**, 1240 (1990).

<sup>8</sup> Jed Dempsey and B. I. Halperin, *Phys. Rev. B* **45**, 3902 (1992); **47**, 4662 (1993).

<sup>9</sup> Jed Dempsey and B. I. Halperin, *Phys. Rev. B* **47**, 4674 (1993).

<sup>10</sup> T. Ando, *J. Phys. Soc. Jpn.* **44**, 475 (1978).

<sup>11</sup> F. Stern and S. Das Sarma, *Phys. Rev. B* **30**, 840 (1984).

<sup>12</sup> M. P. Stopa and S. Das Sarma, *Phys. Rev. B* **45**, 8526 (1992); **47**, 2122 (1993).

<sup>13</sup> T. Ando, A. B. Fowler, and F. Stern, *Rev. Mod. Phys.* **54**, 437 (1982).

<sup>14</sup> W. G. Teich and G. Mahler, *Phys. Status Solidi B* **138**, 607 (1986).

<sup>15</sup> H. D. Drew (private communication).

<sup>16</sup> Jed Dempsey and B. I. Halperin, *Phys. Rev. B* **45**, 1719 (1992).

<sup>17</sup> Norman J. Horing, *Ann. Phys. (N.Y.)* **31**, 1 (1965); M. J. Stephen, *Phys. Rev.* **129**, 997 (1963).

<sup>18</sup> L. I. Magarill and A. V. Chaplik, *Pis'ma Zh. Eksp. Teor. Fiz.* **40**, 301 (1984) [*JETP Lett.* **40**, 1089 (1984)].

<sup>19</sup> P. I. Tamborenea and S. Das Sarma, *Solid State Commun.* **89**, 1009 (1994).